BTO 2013.048 | September 2013

BTO rapport

Fate of fullerenes in water

KWR Watercycle Research Institute

BTO Rapport

Fate of fullerenes in water

Colloidal stability of (functionalised) fullerenes in the presence of dissolved organic carbon and electrolytes

BTO 2013.048 | July 2013

Project number
B222022 and S308646

Project manager
Merijn Schriks

Client
BTO

Quality Assurance
Pim de Voogt

Author(s)
Joris J.-H. Haftka, Erik Emke, Patrick S. Bäuerlein, Annemarie van Wezel, and Thomas L. ter Laak

Sent to
This report has been distributed among BTO-participants and is publicly available

Year of publishing
2013

More information
T +31 6 25243017
E Thomas.ter.laak@kwrwater.nl

PO Box 1072
3430 BB Nieuwegein
The Netherlands

T +31 (0)30 60 69 511
F +31 (0)30 60 61 165
E info@kwrwater.nl
I www.kwrwater.nl

KWR Watercycle Research Institute

Voorwoord

Het voorliggende onderzoek is uitgevoerd in het kader van het bedrijfstakonderzoek van de Nederlandse drinkwaterbedrijven (BTO) en van het grote FES NanonextNL. De Nederlandse overheid investeert via NanonextNL significant met 125 miljoen euro om ontwikkeling, toepassing en inzicht risico's van nanotechnologie te bevorderen. In NanoNextNL werken meer dan 100 commerciële bedrijven, 13 universiteiten, 6 academische ziekenhuizen en 9 technologische instituten samen. Het voorliggende onderzoek is onderdeel van het thema 'Risk Assessment and Technology Assessment' binnen NanonextNL, waarin onder andere de risico's van de nanotechnologische ontwikkelingen voor mens en milieu worden onderzocht. Voor het inschatten van deze risico's is informatie over het gedrag van deze materialen in de waterzuivering en de verdere waterketen van groot belang. Tot op heden is hierover echter nog weinig bekend. Naast de Themagroep Nieuwe stoffen vanuit BTO buigt ook de Stichting NanonextNL en AgentschapNL zich namens de Nederlandse Overheid (Economische Zaken, Landbouw en Innovatie) over de resultaten.

In de voorliggende studie is het gedrag van fullerenen (organische nanomaterialen) in waterige matrices onder invloed van zouten en humuszuren onderzocht. Kennis van het gedrag van deze deeltjes in water is essentieel om te begrijpen en om te voorspellen of en hoe deze deeltjes zich in het aquatisch milieu verspreiden, en in hoeverre verschillende zuiveringstechnieken een barrière voor deze deeltjes vormen. Hoofdstuk 4, 'Potential implications for drinking water sources and production', schenkt specifiek aandacht aan de relevantie van deze studie voor de drinkwatersector.

Samenvatting

Koolstof nanodeeltjes, zoals fullerenen, maken dat ze veelvuldig toegepast in persoonlijke verzorgingsproducten, medicijnen, en zonnecellen. De eigenschappen van geproduceerde nanodeeltjes worden op steeds grotere schaal onderzocht vanwege toepassingen, maar ook vanwege hun mogelijke risico's voor mens en milieu. Veel studies naar de risico's van nanodeeltjes zijn gericht op C_{60}, terwijl in commerciële toepassingen zoals zonnecellen vooral gefunctionaliseerde fullerenen worden gebruikt omwille van hun betere oplosbaarheid in oplosmiddelen en elektrische eigenschappen. Er is een gebrek aan informatie over de eigenschappen en het gedrag in het milieu van deze gefunctionaliseerde fullerenen. Het is daarom van belang dat naast C_{60} ook het gedrag van gefunctionaliseerde fullerenen in waterige matrices met verschillende eigenschappen wordt onderzocht. In deze studie is de colloïdale stabiliteit van C_{60} en [6,6]-diphenyl-C_{62}-bis(butyric acid methyl ester) onder invloed van humuszuren en zouten (NaCl and $CaCl_2$) bestudeerd in een statisch experiment. De concentraties van fullerenen in suspensie zijn bepaald met vloeistofchromatografie gekoppeld aan een Orbitrap massaspectrometer. De deeltjesgrootte van de aggregaten is bepaald met verschillende lichtverstrooiingstechnieken en bleek ongeveer 200 nm zonder toevoeging van zout en humuszuur. De toevoeging van zout leidde tot de vorming van grotere aggregaten. Bovendien bleek het bivalente kation Ca^{2+} een sterker effect op de deeltjesgrootte te hebben dan het monovalente Na^{+}. Daarnaast bleek het toevoegen van relatief lage concentraties humuszuur (2 mg C/L) in combinatie met NaCl de aggregaten in suspensie te stabiliseren. De combinatie van humuszuren en $CaCl_2$ leidde echter tot de precipitatie van de humuszuren en daarmee ook tot co-precipitatie van de fullerenen. Deze resultaten laten zien dat (gefunctionaliseerde) fullerenen waarschijnlijk relatief makkelijk precipiteren in natuurlijke watersystemen, omdat lage concentraties humuszuren en gehalten van Ca^{2+} al leiden tot precipitatie van humuszuren en co-precipitatie van fullerenen. Dit betekent dat flocculatie, een techniek die veelvuldig toegepast wordt in de waterzuivering, mogelijk een geschikt middel is om eventueel aanwezige (gefunctionaliseerde) fullerenen uit het water te verwijderen.

Summary

Carbon-based nanoparticles such as fullerenes have been widely applied in personal care products, drug delivery systems, and solar cells. The properties of nanoparticles have been increasingly studied because of their applications and their potential risks to the environment and human health. Many studies have focused on the environmental fate and properties of C_{60}. However, there is currently limited information available on the environmental properties of functionalised fullerenes. It is therefore considered relevant to study the environmental fate of fullerenes derivatives as a function of the solution chemistry in order to mimic the natural environment and conditions in water treatment systems. The colloidal stability of two fullerenes (C_{60} and [6,6]-diphenyl-C_{62}-bis(butyric acid methyl ester)) in water was studied in the presence of dissolved organic carbon (DOC) and different electrolytes (NaCl and $CaCl_2$). Suspended fullerene concentrations were determined with high resolution Orbitrap mass spectrometry. Aggregate size of the fullerenes was measured with different light scattering techniques. Size measurements showed increasing particle sizes of both fullerenes in the presence of electrolytes with a larger influence of divalent compared to monovalent inorganic cations. The suspended concentrations of the fullerenes were stabilised by low concentrations of DOC (2 mg C/L) if NaCl is present as electrolyte. However, precipitation of DOC occurred at low concentrations of $CaCl_2$ in solution which caused co-precipitation of (functionalised) fullerenes. The results suggest that (functionalised) fullerenes can precipitate in natural aqueous systems at low concentrations of DOC and multivalent inorganic electrolytes.

Contents

1 Introduction

Carbon-based nanoparticles such as fullerenes and their functionalised forms have been used in personal care products [1], in biomedical applications such as drugs delivery systems in cancer therapy [2], and in electronic applications as an *n*-type semiconductor in polymer composites in organic photovoltaic cells [3]. Fullerenes also occur as a result of natural processes, see references cited in Isaacson et al. [4]. Bare fullerene molecules have their carbon atoms in a symmetrical cage structure consisting of hexagons and pentagons, for C_{60} with a total diameter of about 1 nm [5]. Functionalised fullerenes have been functionalised with polar functional groups to increase their solubility and to improve their electronic properties for application in organic photovoltaic cells. Fullerenes have shown toxic effects in bacteria [6,7], fish [8], and human cell lines [9]. Antibacterial activity was found to be higher for smaller aggregates [7]. Fullerenes exhibit a very low solubility in water (calculated aqueous solubilities of C_{60} are < 8 ng/L) [10,11]. However, upon entering water, fullerenes (as C_{60}) can form stable aqueous suspensions (denoted as nC_{60}) with physicochemical properties that are different from C_{60} in the condensed phase [4]. Water-stable aggregates with negative charge are formed over time with increasing pH [12,13], decreasing ionic strength [12,14], higher initial fullerene concentration [15], and longer storage time [14]. These properties in aqueous solution such as particle size and shape are also dependent on the way of preparing fullerene suspensions, i.e., by extended stirring, sonication, or solvent exchange. Sonication and solvent exchange result in more spherical shapes and a homodisperse size distribution, while extended stirring (for two to seven weeks) leads to more angular shapes and a polydisperse size distribution [12,15]. This has been explained by ordering of small clusters to form new crystals (bottom-up process) in the solvent exchange method, whereas larger aggregates can break down into smaller aggregates (top-down process) in the extended stirring method in addition to the formation of crystals [15].

Aqueous suspensions of fullerenes naturally obey aggregation behaviour according to the classic theory of colloidal stability from Derjaguin-Landau-Verwey-Overbeek. According to this theory, the attractive and repulsive interactions between (spherical) colloids are dominated by both van der Waals forces and electrostatic double layer forces [16]. The stability of colloidal particles in water is determined by the balance between these forces that are determined by both chemical composition and ionic strength in a solution. The electrostatic double layer surrounding colloidal particles is extended in solution at low ionic strength, whereas the double layer is compressed at high ionic strength. Compression of the double layer in combination with favourable van der Waals interactions causes colloids to aggregate with subsequent sedimentation of the aggregates. However, variable shape and composition of nanoparticles, and the presence of macromolecular compounds (e.g., natural organic carbon or clays) in the environment complicate the application of this theory [16]. Apart from theoretical considerations, the colloidal stability of fullerene suspensions can be quantified by determination of the critical coagulation concentration (CCC) with dynamic light scattering (DLS). Using time-resolved DLS, the aggregation kinetics of fullerene suspensions with increasing electrolyte concentrations can be expressed as attachment efficiency, α. The transition from slow aggregation (reaction-limited regime) to fast aggregation (diffusion-limited regime) is defined as the CCC value for a specific type of electrolyte. When the electrolyte concentration reaches the CCC value, the surficial charges are effectively reduced in strength and van der Waals interactions dominate which lead to fast aggregation rates. Faster aggregation rates of fullerenes will influence sedimentation

rates and their subsequent removal from water [17]. Divalent electrolytes obviously result in lower CCC values for nC_{60} colloids compared to monovalent electrolytes [12]. Enhanced aggregation of fullerenes is observed in the presence of both $CaCl_2$ and dissolved organic carbon (DOC = 1 mg C/L of Suwannee river humic acid). This was attributed to intermolecular bridging via complexation of Ca^{2+} with DOC which subsequently promoted aggregation of fullerenes [18].

Differences in preparation methods, presence of organic carbon, or photochemical alteration can result in differences in the colloidal stability of fullerenes. Fullerene suspensions produced by the extended stirring method show a CCC value (determined with KCl) that is about a factor of 4 higher compared to a fullerene suspension produced by sonication. This was explained by the higher charge (zeta potential) of fullerenes produced by surface oxidation reactions during extended stirring [12]. Likewise, CCC values of fullerenes (determined with NaCl) increase by a factor of 3.9 and 7.4 due to the presence of 1 mg/L Suwannee river humic acid and irradiation for 7 days by UV light at 350 nm, respectively. Hydrophobic interactions between Suwannee river humic acid and fullerenes stabilize the fullerene suspension [19] with smaller particles observed in the presence of DOC [20]. The increased stability of fullerene suspensions that are irradiated with UV light is caused by surface modifications of fullerenes such as the introduction of oxygen containing functional groups [19]. The CCC value of a functionalised fullerene such as [6,6]-phenyl-C_{61}-butyric acid methyl ester increases by a factor of 2.2 compared to aggregation of nC_{60} because the aggregates of the functionalised fullerene have more interactions with water [21].

In summary, the colloidal stability of fullerenes in the environment is affected by a multitude of factors such as ionic strength of the solution and the nature of the ions present, humic acids, and the charge of the fullerenes (zeta potential). A more thorough investigation of relevant factors involved in the stabilization and aggregation of fullerene suspensions in time is required. This information is considered important for an improved understanding and assessment of the environmental fate of fullerenes and thus of the risks that fullerenes can pose to the environment. The aggregation behaviour of fullerenes will be mostly determined by hetero-aggregation with other suspended matter in soil and aqueous solutions [22], such as DOC, particulate organic carbon, clay, or metal oxides. An improved understanding of the factors influencing colloidal stability will also provide more insight in the fate of (functionalised) fullerenes in waste and drinking water treatment plants [23].

There is currently limited information available on the environmental fate of functionalised fullerenes, whether they enter sources of drinking water can pass common treatment techniques. Literature provides some clues. Studies show that sorption coefficients of individual fullerene molecules are extremely high [24]. This suggests that fullerenes strongly sorbed to (organic) environmental matrices probably do not reach drinking water sources as individual molecules. However, fullerenes can form rather stable aggregates in aqueous matrices. These aggregates are more hydrophilic than their individual constituents. These aggregates are mobile in soil and tend to remain in the aqueous phase for long periods of time. Furthermore, various studies show that their mobility in soil and sediment depends on its structure (particles size, composition), the presence of salts in aqueous solution (NaCl, $CaCl_2$), and the presence of humic acids [25, 26]. This suggests that stable fullerene aggregates can enter drinking water sources and advocates for further research on the behaviour of these aggregates in water.

The ionic strength of fullerene suspensions with and without DOC was varied by increasing monovalent and divalent inorganic cation concentrations (NaCl and $CaCl_2$). Aggregate stability is mostly studied by measuring aggregation rates with time-resolved DLS, but there is hardly any data of the fullerene concentrations during the aggregation process. Fullerene concentrations were therefore measured in time with liquid chromatography coupled to high resolution mass spectrometry. In addition, particle size analysis of the suspensions was performed with DLS and asymmetric flow-field-flow fractionation coupled to multi-angle light scattering (AF4-MALS).

2 Material and Methods

2.1 Chemicals

C_{60} (>99.9%; CAS 99685-96-8; *MW* = 720.660 g/mol) was obtained from Materials and Electrochemical Research Corporation (Tucson, AZ). C_{60}PCBM ([6,6]-phenyl-C_{61}-butyric acid methyl ester; >99%; CAS 160848-22-6; *MW* = 910.901 g/mol), and C_{60}BisPCBM ([6.6]-diphenyl-C_{62}-bis(butyric acid methyl ester); >99.5%; CAS 1048679-01-1; *MW* = 1101.143 g/mol) were obtained from Solenne (Groningen, the Netherlands). C_{60}PCBM was used as an internal standard in the LC-MS analysis for the quantification of C_{60} and C_{60}BisPCBM. The molecular structures of the test compounds are shown in Figure 1. Note that C_{60}BisPCBM is a mixture of different isomers due to several possibilities to substitute the side-chain(s) [27]. Inorganic salts (NaCl, $CaCl_2.2H_2O$, NaN_3, and NaOH) were obtained from J.T. Baker (Boom, Meppel, the Netherlands). The organic buffer 3-(N-morpholino)propanesulfonic acid (MOPS) was obtained from Sigma-Aldrich (Zwijndrecht, the Netherlands). Acetone, toluene, and ethanol (HPLC grade) were obtained from J.T. Baker (Biosolve, Valkenswaard, the Netherlands) and petroleum ether (≥ 95%) was obtained from Sigma-Aldrich. Leonardite humic acid containing 63.81% OC was obtained from the International Humic Substances Society (http://www.humicsubstances.org/; St. Paul, MN). Water (resistivity >18 MΩ/cm) was obtained from a Milli-Q water purification system (Millipore, Amsterdam, the Netherlands).

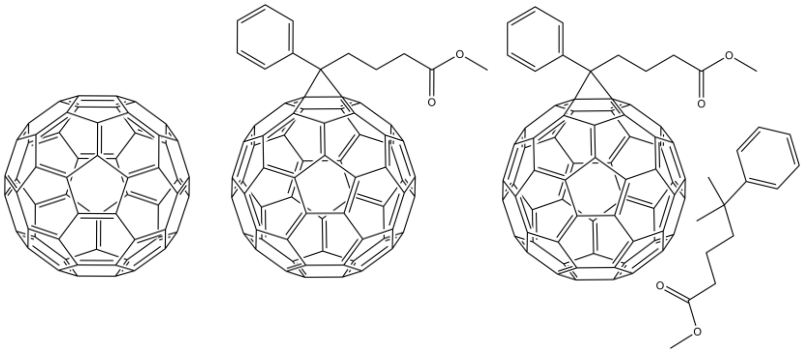

Figure 1. Molecular structures of C_{60}, C_{60}PCBM ($C_{72}H_{14}O_2$) and C_{60}BisPCBM ($C_{84}H_{28}O_4$)

2.2 Preparation of fullerene suspensions

Aqueous suspensions of (individual) fullerenes were made by solvent exchange with toluene. Glass vials of 40 mL (Aurora Borealis Control BV, Schoonebeek, the Netherlands) were filled with 30 mL water and 3 mL ethanol was added to the vials. The vials were placed into an ultrasonic bath (Branson 3210) that was held at a constant temperature of 30 °C. A volume of 0.5 mL (60.32 mg/L C_{60}) or 0.6 mL (61.91 mg/L C_{60}BisPCBM) fullerene solution dissolved in toluene was subsequently infused at 25 μL/min. into the vials. This produced a white emulsion that slowly converted into a transparent solution after 3-4 hours of degassing in the ultrasonic bath. The suspensions were pooled into an Erlenmeyer of 500 mL. The final weight of both suspensions increased by 4% (w/w_ of the initial water volume. This increase was attributed to the presence of residual ethanol in the suspension(s). The solution was filtered through a Whatman GF/C glass fiber membrane filter (Boom; nominal pore size 1.2 μm) and stored at room temperature in the dark. Analysis of the distribution of fullerenes

between vials (*i.e.*, glass surface), filter, and suspension is described in the Supporting Information.

2.3 Preparation of dissolved organic carbon

An amount of 20 mg of Leonardite humic acid was dissolved in 100 mL of water by adjusting to pH 11 with 1 M of NaOH. The solution was stirred overnight and filtered through Pall Gelman polyethersulphone membrane filters (VWR, Amsterdam, the Netherlands; pore size 0.45 μm). Filters were rinsed with about 200 mL of Milli-Q water prior to filtration of the DOC solution. After filtration of 25 mL of DOC, the filter was replaced to prevent clogging of the filter. The concentration of non-purgeable organic carbon was measured with a TOC-VCPH Shimadzu combustion analyzer (Shimadzu, 's Hertogenbosch, the Netherlands). Treatments containing DOC were prepared by adding 0.2 to 4 mL of this stock solution to 20 mL of water.

2.4 Static equilibration of fullerene treatments

In separate experiments for C_{60} and C_{60}BisPCBM, a volume of 5 mL of fullerene suspension was added with a glass pipette in duplicate to 20 mL clear glass vials (VWR) containing 10 mL of DOC or water with final concentrations of 1 mM NaN_3 and 10 mM MOPS (duplicate samples). The pH of the final solution was 6.94 and did not change during the course of the experiments. After 3 hours of equilibration of fullerenes and DOC, the NaCl or $CaCl_2$ solutions were added to the vials and these were shaken by hand. The final electrolyte concentrations with and without DOC (2 mg C/L) were 25, 38, 59, 90, 138, 212, 326, and 500 mM for the NaCl treatments and 0.25, 0.48, 0.93, 1.80, 3.47, 6.71, 12.95, and 25 mM for the $CaCl_2$ treatments. Treatments containing no electrolytes, 25 mM NaCl, and 0.93 mM $CaCl_2$, respectively, were sampled in time (7 sampling times within 33 days for *n*C_{60} and 5 sampling times within 23 days for *n*C_{60}BisPCBM) to study the time dependence of the colloidal stability of both fullerenes in the presence or absence of DOC.

After static equilibration for 3 days at room temperature in the dark, samples of 2 mL were withdrawn from the upper layer for all treatments. Liquid-liquid extraction (LLE) was subsequently performed by adding 3 mL of toluene and 1 mL of 30 g/L NaCl solution. NaCl was added to the solutions to aid in the recovery of the fullerene(s). An internal standard of 50 μL of C_{60}PCBM dissolved in toluene was added to the toluene phase (final concentration of 8.93 μg/L) for quantification of the fullerenes. The vials were shaken horizontally at 200 rpm for 30 minutes. A volume of 1 mL of the toluene phase was subsequently sampled and the samples were stored at 4°C prior to LC-Orbitrap MS analysis.

The effect of DOC on the extraction recovery of both fullerenes with LLE was studied with relevant environmental DOC concentrations of 1, 2, 5, 10, and 20 mg C/L. Sequential extraction of *n*C_{60} was tested for samples without DOC and with 2 and 20 mg C/L. Only 1% of C_{60} was found in the second extraction step for the samples without DOC and with 2 mg C/L, whereas 2 to 3% was found in the second and third extraction of the sample containing 20 mg C/L. No C_{60} could be recovered in the third extraction step with toluene of the sample with 2 mg C/L, while the sample with 20 mg C/L could not be extracted for a third time because of emulsification of the toluene-water interface. All subsequent LC-Orbitrap MS measurements of LLE samples were therefore performed by taking 1 mL from the first extraction with toluene. The extraction recovery of *n*C_{60} and *n*C_{60}BisPCBM for samples with DOC concentrations ranging from 1 to 20 mg C/L is shown in Figures S1 (percentages) and S2 (concentrations). Recoveries of samples at relatively low concentrations of DOC were close to 100% and no corrections for recovery were therefore applied in subsequent experiments.

C_{60}BisPCBM showed a lower recovery of about 90% at the highest DOC concentration tested (no corrections were applied here). This was probably due to stronger interactions of the side-chains of C_{60}BisPCBM with DOC.

2.5 Liquid chromatography coupled to mass spectrometry

A detailed description of the analysis and detection of several functionalised fullerenes (also including C_{70}) can be found in Kolkman et al [27]. Quantification was based on the sum of the peak areas of the accurate masses (within a 5 ppm mass window) of the fullerene compound and all its related adducts [28]. Calibration curves of C_{60} and C_{60}BisPCBM were linear in the range of 0 to 32 μg/L. The detection limits were 0.22 μg/L for C_{60}BisPCBM and 0.33 μg/L for C_{60}.

2.6 Flow-field-flow fractionation

Samples from the stock suspension of fullerene(s) were measured with a Postnova AF2000 system (Postnova Analytics GmbH, Landsberg, Germany) consisting of an asymmetric flow-field-flow fractionation (AF4) module coupled to a UV detector (Shimadzu) and a multi angle light scattering detector (MALS; Postnova). A volume of 100 μL of sample was injected into a thin channel of water flowing over a membrane (10 kDa regenerated cellulose, Postnova) with Milli-Q as eluent. At the moment of injection, the sample was focused into a small laminar band by opposing flows. After the focus flow of 1 mL/min. stopped after 5 min., the cross-flow (1 mL/min.) exponentially decreased to 0.1 mL/min. at 46 min. resulting in a higher retardation of large size components. The obtained size distributions were analysed with Postnova software program version 1.1.0.31. A short explanation of the AF4-MALS measurements is given in the Supporting Information.

2.7 Dynamic light scattering and electrophoretic mobility

The hydrodynamic diameter was measured with DLS using a NanoZS Zetasizer from Malvern instruments equipped with a He-Ne laser operating at 633 nm. Scattered light intensities were measured at an angle of 173° and a refractive index of 2.20 [29] was used for nC_{60} and nC_{60}BisPCBM in these measurements. The size distributions were analysed with Malvern Dispersion Technology Software version 5.10. The zeta potential or electrophoretic mobility was also determined with a NanoZS Zetasizer in folded capillary cells (Malvern).
The particle size and electrophoretic mobility measurements were all made with the stock suspensions of nC_{60} (441 μg/L) and nC_{60}BisPCBM (718 μg/L), unless noted otherwise. A short description of the measurements of particle diameter and electrophoretic mobility is given in the Supplemental Data.

3 Results and Discussion

3.1 Characterization of particles

The particle size distribution of the fullerene suspensions prepared via solvent exchange in the absence of electrolytes was measured with DLS and AF4-MALS for *n*C_{60} (Figure 2a) and *n*C_{60}BisPCBM (Figure 2B). The particle size distribution of *n*C_{60} measured with DLS showed a broader distribution compared to that of AF4-MALS. In the DLS technique, diffusion coefficients are measured from intensity fluctuations of scattered light in the order of micro- to milliseconds due to Brownian motion of the particles. The hydrodynamic diameter is subsequently derived from these diffusion coefficients. In the MALS technique, the intensity of scattered light is averaged over time in the order of 0.01 to 0.1 seconds and is related to the absolute molar mass that gives a root mean square radius (or radius of gyration) of the particles. Note that the hydrodynamic diameter is measured with DLS, which includes solvent molecules that move with the particle. This would therefore explains the broader size distribution measured with DLS (hydrodynamic diameter) compared to MALS (exact diameter). The maximum scattering intensities measured with both techniques were similar for nC_{60}, see Figure 2A. The hydrodynamic diameter at maximum intensity of nC_{60} was close to the diameter based on the Z-average (intensity-weighted average) calculated with the DLS software, see Table 1. However, the hydrodynamic diameter at maximum intensity of nC60BisPCBM measured with DLS was significantly smaller compared to the particle diameter measured with AF4-MALS (Student's t-test assuming equal variances and normal distribution of data; $p < 0.05$), see Figure 2B. This discrepancy in measured particle diameters may be explained by the used refraction index increment that was assumed to be similar for C_{60} and C_{60}BisPCBM. The refraction index was used as an input parameter in the calculation of the particle size with MALS. However, the refraction index was only known for C_{60} and the same value was used for C_{60}BisPCBM. Differences in molecular size and shape of C_{60} and C_{60}BisPCBM might also explain the observed size differences of the aggregates. The particle diameters determined for the nC_{60} suspension were in agreement to intensity-weighted averages from the literature that were determined for suspensions of nC_{60} prepared by either solvent exchange (*d* = 90 to 219 nm) [6,12,15,30-32], sonication (*d* = 166 nm) [19] or extended stirring methods (*d* = 171 to 193 nm) [12,15,21,31,33]. A literature value for the particle diameter of a functionalised fullerene (*d* = 186 for nC_{60}PCBM) prepared by extended stirring for 5 months [21] is also in close agreement with the values for nC_{60}BisPCBM determined in this study.

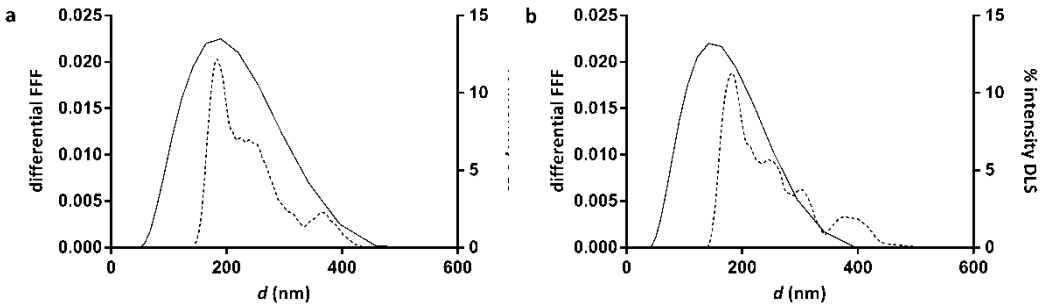

Figure 2. Particle size distribution of nC_{60} (Figure 2a) and nC_{60}BisPCBM (Figure 2b) measured with dynamic light scattering (closed line) and AF4-multi angle light scattering (dashed line).

Table 1. Particle diameters (d ± SD) based on maximum or Z-averaged intensity measured with dynamic light scattering (DLS) and multi-angle light scattering (MALS). The zeta potential (ζ ± SD) is measured with phase analysis light scattering (PALS). Numbers in parentheses indicate the number of measurements.

Sample	Treatment	d_{max} (in nm) MALS	d_{max} (in nm) DLS	d_Z (in nm) DLS	ζ (in mV) PALS
nC_{60}	Control	178 ± 13 (3)	185 ± 4 (4)	174 ± 5 (4)	-41 ± 1 (3)
	100 mM NaCl	-	243 ± 5 (3)	180 ± 5 (3)	Nd
	10 mM $CaCl_2$	-	811 ± 52 (4)	1295 ± 52 (4)	Nd
nC_{60}BisPCBM[a]	Control	182 ± 3 (3)	154 ± 2 (4)	151 ± 5 (4)	-53 ± 1 (3)
	100 mM NaCl	-	227 ± 14 (4)	187 ± 9 (4)	nd

a The sample of nC60BisPCBM at 10 mM CaCl2 was too polydisperse for a reliable measurement with DLS.

The particle diameters of nC_{60} and nC_{60}BisPCBM were also measured with both techniques in the presence of either NaCl or $CaCl_2$, see Table 1. The particle size of the solutions containing electrolytes could only be measured with DLS, because the signal measured with AF4-MALS quickly diminished (Supplemental Data, Figure S2 and S3). The apparent loss of fullerenes from solution and associated low signal intensity prevented a reliable determination of the particle size. The peaks seemed to shift to longer retention times in the case of NaCl and to shorter retention times for $CaCl_2$ treatments. The particle diameter measured with DLS for both nC_{60} and nC_{60}BisPCBM with 100 mM NaCl showed an increase by a factor of 1.3 to 1.5, see Table 1. The particle size of nC_{60} aggregates in the presence of 10 mM $CaCl_2$ increased by a factor of 4.4 compared to the control treatment without electrolytes. However, the particle size of aggregates in the $CaCl_2$ treatments could only be measured for nC_{60}, because nC_{60}BisPCBM showed a particle size distribution that was too polydisperse to be reliably quantified. The presence of DOC (1 mg C/L) did not affect the particle size distribution and intensity of nC_{60} (Supplemental Data, Figure S4). The measured zeta potential of nC_{60} and nC_{60}BisPCBM was negative (see Table 1) and was in a similar range as literature values (-47 to -30 mV) for nC_{60} prepared by solvent exchange and sonication [12,31,32].

3.2 Time dependence of colloidal stability

The concentrations of nC_{60} were followed in time for the treatments containing 25 mM NaCl and 0.9 mM $CaCl_2$, see Figure 3A. The concentrations of nC_{60} measured in the NaCl and $CaCl_2$ treatments in the absence of DOC significantly decreased to 79 and 72 % ($p < 0.05$), respectively, of the original value after 33 days. Half-lives of nC_{60} due to settling, calculated via first-order exponential decay, amounted to 61±4 days for the NaCl treatment and 93±9 days for the $CaCl_2$ treatment. Settling obviously occurred because monovalent and divalent electrolytes increase the aggregate size of nC_{60} colloids. However, concentrations of nC_{60}BisPCBM in treatments containing the same electrolyte concentrations without DOC were not affected over a period of 23 days ($p > 0.05$), see Figure 3B. Colloids of nC_{60}BisPCBM seemed to be more stable compared to nC_{60} colloids irrespective of the larger aggregate size of nC_{60}BisPCBM in the presence of monovalent electrolytes, see Table 1. The treatments of nC_{60} and nC_{60}BisPCBM containing both electrolytes and DOC did not show any significant decrease (Supplemental Data, Figure S5 and S6). Previously, smaller aggregate sizes of nC_{60} were observed in the presence of Suwannee river humic acid suggesting that humic acid sterically stabilized suspensions of nC_{60} [20,33]. The stability of the fullerene concentrations in the DOC treatments shows the ability of a relatively low DOC concentration (2 mg C/L) to stabilize nC_{60} and nC_{60}BisPCBM colloids in aqueous solutions for prolonged periods of time.

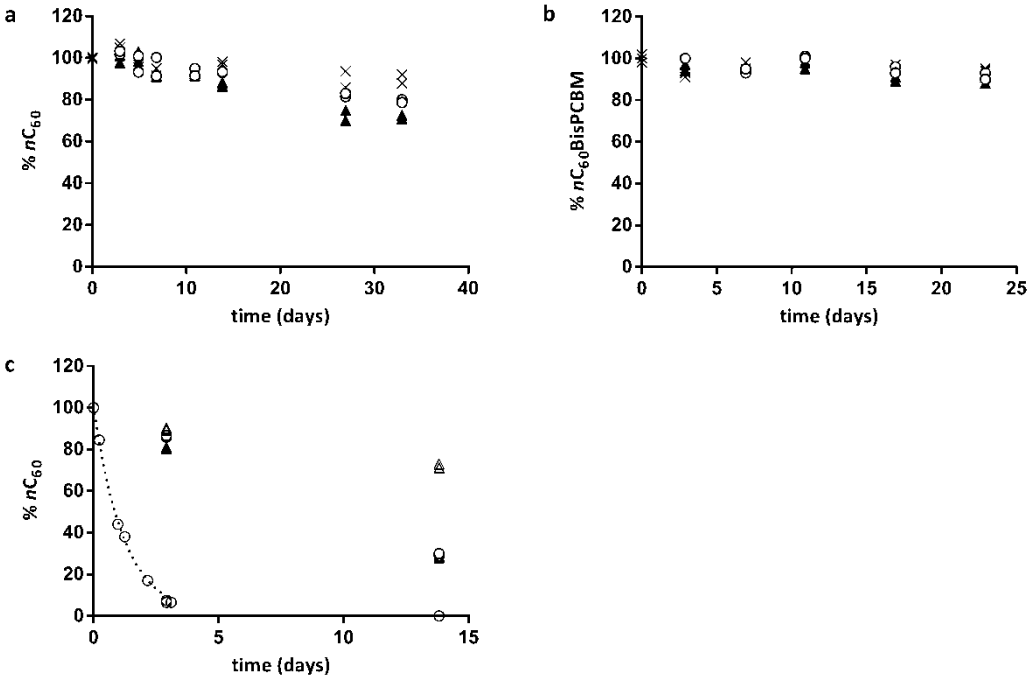

Figure 3. Percentage of nC_{60} (Figures 3A and C) and nC_{60}BisPCBM (Figure 3B) as a function of time. Crosses represent data for control solutions without salt or DOC. Closed and open triangles represent treatments with NaCl and NaCl+DOC, respectively (25 mM in Fig. 3A and 3B and 500 mM in Figure 3C). Closed and open circles represent treatments with $CaCl_2$ and $CaCl_2$+DOC, respectively (0.93 mM in Figure 3A and 3B and 25 mM in Fig. 3C).

Concentrations of nC_{60} in treatments containing 500 mM NaCl and 25 mM $CaCl_2$ in the absence of DOC were measured after 3 and 14 days. The treatments containing 500 mM NaCl and DOC showed a strong reduction of the nC_{60} concentrations to ~28% from 3 to 14 days (see Figure 3C), whereas the nC_{60} concentrations were not affected at 25 mM NaCl and DOC (Supplemental Data, Figure S5). Aggregation and subsequent precipitation of nC_{60} from solution in the presence of monovalent electrolytes presumably takes weeks to even months at natural freshwater DOC and electrolyte concentrations. Co-precipitation of nC_{60} with DOC in treatments containing 25 mM $CaCl_2$ was however a very fast process (half-life of 0.85±0.04 days fitted via exponential decay, see Figure 3C) with only 6 to 8% residual nC_{60} suspended in solution after 3 days and an absence of nC_{60} in solution after 14 days. This process occurred because of formation of DOC aggregates by intermolecular bridging via calcium complexation [18]. Subsequent sorption of nC_{60} to the formed DOC aggregates resulted in rapid removal of nC_{60} from the aqueous phase. Sedimentation of fullerenes in the absence of DOC seemed to be an on-going process, see Figure 3C for treatments without DOC. However, a period of 3 days was selected as incubation time for the measurement of fullerene concentrations in all electrolyte and electrolyte+DOC treatments because this period is considered a relevant environmental timeframe as residence times of water in rivers often range from several days to one month while timeframes in waste water and drinking water treatment systems range from hours to day(s) for the full treatment process. Despite the differences in physico-chemical properties between nC_{60} and nC_{60}BisPCBM both compounds show grosso modo a comparable behaviour towards the influence of electrolyte and DOC

3.3 Effect of electrolytes and DOC on colloidal stability

The effect of NaCl (25-500 mM) on the concentrations of nC_{60} and nC_{60}BisPCBM after a static equilibration time of 3 days is shown in Figure 4A. The NaCl concentrations covered the range of concentrations of monovalent electrolytes in Dutch riverwater (c_{Na+K} = 0.95-4.07 mM; river Meuse, averaged over 2001-2011, [34]) and in seawater (c_{Na+K} = 479 mM). Both fullerenes appeared to be stabilized by the presence of DOC with NaCl as electrolyte. Fullerene concentrations were slightly higher in the DOC treatments compared to the treatments without DOC. The stabilization of fullerenes by DOC is explained by sorption of fullerenes to DOC in solution (Klavins and Ansone, 2010), whereas more extensive sedimentation and/or glass wall sorption results in lower fullerene concentrations in the treatments without DOC. The DOC source used was a commercial humic acid which is one of the most hydrophobic humic acids that is currently available [35]. Recently, measurements of fullerene settling over a 1-year period with 4 natural DOC samples (hardness, $[Ca^{2+}+Mg^{2+}]$ = 0.10-0.33 mM) indicated that a higher colloidal stability of nC_{60} correlated with more hydrophobic DOC [36]. This suggests that molecular properties of DOC such as aromaticity are important in the interactions between DOC and fullerenes. The relatively high hydrophobicity of the DOC source used in this study is probably responsible for the sorption and subsequent stabilization of fullerenes at already relatively low DOC concentrations (2 mg C/L). In the treatments of 500 mM NaCl without DOC, fullerene concentrations significantly decreased to 81% for nC_{60} and 90% for nC_{60}BisPCBM compared to the stock concentrations (p < 0.01), see Figure 3C. In the treatments with DOC, fullerene concentrations decreased to 90% for nC_{60} and 91% for nC_{60}BisPCBM (p < 0.04).

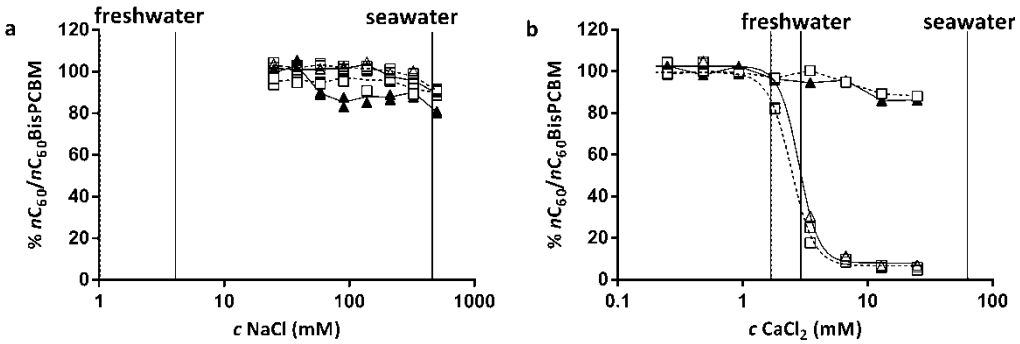

Figure 4. Effect of NaCl (Figure 4a) and $CaCl_2$ (Figure 4b) on the concentrations of nC_{60} (straight lines) and nC_{60}BisPCBM (dashed lines) with and without 2 mg C/L DOC. Closed and open triangles represent data for nC_{60} and nC_{60}+DOC, respectively. Closed and open squares represent data for nC_{60}BisPCBM and nC_{60}BisPCBM+DOC, respectively. Note that the x-axis has a logarithmic scale.

The effect of $CaCl_2$ (0.25-25 mM) on the concentrations of nC_{60} and nC_{60}BisPCBM after a static equilibration time of 3 days is shown in Figure 4B. The highest $CaCl_2$ concentrations used were about 12 times higher than the concentrations of divalent electrolytes in the river Meuse (c_{Ca+Mg} = 1.66-3.01 mM; averaged over 2001-2011), but were lower than the concentration present in seawater (c_{Ca+Mg} = 63 mM). The concentration of nC_{60} in the $CaCl_2$ treatment without DOC decreased to 86% (P < 0.01) of the initial concentration, whereas the decrease in the concentration of nC_{60}BisPCBM was not significant. However, the concentrations of nC_{60} and nC_{60}BisPCBM at the higher $CaCl_2$ concentrations in the presence of DOC plummeted to 7 and 5% of the stock concentration, respectively. This decrease apparently occurred because of precipitation of DOC by complexation with Ca^{2+} [18].

Complexation of Ca^{2+} with DOC reduces the charge on DOC hence promoting aggregation and precipitation. In contrast, monovalent electrolytes such as Na^{+} only function as charge screening counterions [37]. Precipitation of DOC caused co-precipitation of the suspended fullerenes, suggesting that fullerenes and DOC strongly interact. Concentrations of nC_{60} decreased from 95% at 1.80 mM $CaCl_2$ to 31% at 3.74 mM $CaCl_2$, whereas nC_{60}BisPCBM decreased from 82% at 1.80 mM $CaCl_2$ to 21% at 3.74 mM $CaCl_2$. When fitting the data for both fullerenes with a sigmoidal curve, there was no significant difference ($p > 0.05$) in the $CaCl_2$ concentrations at 50% decrease between both tested fullerenes (see Figure 4B).

3.4 Environmental implications

The colloidal stability of fullerene suspensions will likely depend on the intrinsic properties of the (functionalised) fullerenes [17], and will determine the distribution, persistence, and bioavailability of these compounds in the aqueous environment. Both heteroaggregation with natural colloids (such as inorganic metal oxides, organic matter and clay minerals) and solution chemistry (e.g., pH, ionic strength) will ultimately determine the fate and transport of (functionalised) fullerenes in the environment [12,17]. Knowledge of the colloidal stability is therefore important to assess the environmental risks of these compounds in the aquatic environment as well as for adopting appropriate removal strategies in waste and drinking water treatment. For example, literature data show that nC_{60} was efficiently removed from water with coagulation/ flocculation, but removal of the far more hydrophilic and soluble fullerene derivative fullerol ($C_{60}(OH)_{24}$) was less efficient [5].

Currently, mathematical modelling of the exposure of nanoparticles in the environment depends on the direct availability of both concentrations and aggregation state of nanomaterials [38]. Reliable information on environmental exposure data of functionalised fullerenes is therefore required. An accurate time-dependent model of fullerene sedimentation should include DOC and other environmental sorbent concentrations as well as information about temperature, pH, ionic strength, and type of ions present in solution. Measurement of the critical coagulation concentration of functionalised fullerenes in the presence of monovalent to trivalent inorganic cations and DOC sources provides more mechanistic understanding of the relevant molecular properties involved in heteroaggregation of both nanoparticles and organic colloids [39]. In addition, measurement of sedimentation rates of functionalised fullerenes in settling experiments will give more information on the removal kinetics, fate, and exposure concentrations of nanoparticles in the aquatic environment [40,41].

4 Potential implications for drinking water sources and production

Water treatment for the production of drinking water consists of combinations of various treatments. The combination of treatment techniques depends on the nature and the quality of the source. Commonly applied treatments are soil passage (with or without active infiltration), flocculation, aeration, sand filtration, activated carbon treatment, various types of membrane filtration and oxidative processes such as UV disinfection, ozonation or UV-H_2O_2 oxidation. It is largely unknown whether fullerenes and their derivatives can enter sources of drinking water, and if so whether the abovementioned techniques are able to remove them. The current study covers the effect of a limited set of parameters on the colloidal stability of fullerenes in a batch set-up. Nevertheless the current results provide some information that can direct future research on organic nanomaterials in water treatment.

This study has shown that different size characterization methods, i.e., dynamic light scattering and multi-angle light scattering, resulted in particle diameters of nC_{60} and nC_{60}BisPCBM suspensions of about 150-190 nm. A single fullerene is just over one nanometer in diameter, so these aggregates contain in the range of 10^6 individual fullerenes. Although these methods gave slightly different aggregate sizes of (functionalised) fullerene colloids, they are both considered suitable to measure (average) particle diameters of fullerene aggregates in water. Information on the aggregation size is relevant for the behaviour of fullerene aggregates in water treatment using membrane techniques.

The presence of monovalent and divalent electrolytes in water increased the aggregate size of nC_{60} colloids. Electrolyte concentrations at or above seawater levels will finally lead to sedimentation from the aqueous phase. However, analysis of fullerene aggregates at electrolyte concentrations commonly found in fresh water lead to rather stable aggregates and limited sedimentation. Furthermore, the presence of DOC at levels commonly found in groundwater and surface water lead to the formation of stable aggregates of (functionalised) fullerenes. However, the presence of both DOC and divalent electrolytes lead to fast precipitation of DOC-fullerene complexes. This suggests that the humic acids and fullerenes form hetero-aggregates that precipitate due to coagulation when divalent cations are added. Enhanced (co)precipitation of fullerenes can be beneficial in drinking water preparation when coagulation is applied as a water treatment step as results suggest that flocculation processes might be suitable to remove fullerene aggregates from water. The current study was not performed using commonly applied coagulants and ambient humic materials. However, our results are e first step towards the assessment of the behaviour of fullerenes in water and more specifically in flocculation processes.

Future studies can be extended towards natural systems and various treatment processes to assess the fate in the environment and water treatment and might include the measurement of concentrations and aggregation rates of more polar, functionalised fullerenes and the effects of a greater variety of ionic species and natural colloids.

5 Literatuur

1. Woodrow Wilson International Center for Scholars, Project on Emerging Technologies, http://www.nanotechproject.org/inventories/consumer. *December 2012.*
2. Chen, Z.; Mao, R.; Liu, Y. Fullerenes for cancer diagnosis and therapy: Preparation, biological and clinical perspectives. *Curr. Drug Metab.* **2012,** *13,* 1035-1045.
3. Brabec, C. J.; Gowrisanker, S.; Halls, J. J. M.; Laird, D.; Jia, S.; Williams, S. P. Polymer-fullerene bulk-heterojunction solar cells. *Adv Mater* **2010,** *22,* 3839-3856.
4. Hyung, H.; Kim, J. Dispersion of C_{60} in natural water and removal by conventional drinking water treatment processes. *Water Res.* **2009,** *43,* 2463-2470.
5. Fortner, J.; Lyon, D.; Sayes, C.; Boyd, A.; Falkner, J.; Hotze, E.; Alemany, L.; Tao, Y.; Guo, W.; Ausman, K.; Colvin, V.; Hughes, J. C_{60} in water: Nanocrystal formation and microbial response. *Environ. Sci. Technol.* **2005,** *39,* 4307-4316.
6. Lyon, D. Y.; Adams, L. K.; Falkner, J. C.; Alvarez, P. J. J. Antibacterial activity of fullerene water suspensions: Effects of preparation method and particle size. *Environ. Sci. Technol.* **2006,** *40,* 4360-4366.
7. Oberdörster, E. Manufactured nanomaterials (Fullerenes, C_{60}) induce oxidative stress in the brain of juvenile largemouth bass. *Environ. Health Perspect.* **2004,** *112,* 1058-1062.
8. Sayes, C.; Fortner, J.; Guo, W.; Lyon, D.; Boyd, A.; Ausman, K.; Tao, Y.; Sitharaman, B.; Wilson, L.; Hughes, J.; West, J.; Colvin, V. The differential cytotoxicity of water-soluble fullerenes. *Nano Lett.* **2004,** *4,* 1881-1887.
9. Heymann, D. Solubility of fullerenes C-60 and C-70 in seven normal alcohols and their deduced solubility in water. *Fullerene Sci Technol* **1996,** *4,* 509-515.
10. Jafvert, C. T.; Kulkarni, P. P. Buckminsterfullerene's (C_{60}) octanol-water partition coefficient (K_{ow}) and aqueous solubility. *Environ. Sci. Technol.* **2008,** *42,* 5945-5950.
11. Isaacson, C. W.; Kleber, M.; Field, J. A. Quantitative analysis of fullerene nanomaterials in environmental systems: A critical review. *Environ. Sci. Technol.* **2009,** *43,* 6463-6474.
12. Chen, K. L.; Elimelech, M. Relating colloidal stability of fullerene (C_{60}) nanoparticles to nanoparticle charge and electrokinetic properties. *Environ. Sci. Technol.* **2009,** *43,* 7270-7276.
13. Ma, X.; Bouchard, D. Formation of aqueous suspensions of fullerenes. *Environ. Sci. Technol.* **2009,** *43,* 330-336.
14. Brant, J.; Lecoanet, H.; Wiesner, M. Aggregation and deposition characteristics of fullerene nanoparticles in aqueous systems. *J. Nanopart. Res.* **2005,** *7,* 545-553.
15. Duncan, L. K.; Jinschek, J. R.; Vikesland, P. J. C_{60} colloid formation in aqueous systems: Effects of preparation method on size, structure, and surface, charge. *Environ. Sci. Technol.* **2008,** *42,* 173-178.
16. Hotze, E. M.; Phenrat, T.; Lowry, G. V. Nanoparticle aggregation: Challenges to understanding transport and reactivity in the environment. *J. Environ. Qual.* **2010,** *39,* 1909-1924.
17. Chen, K. L.; Smith, B. A.; Ball, W. P.; Fairbrother, D. H. Assessing the colloidal properties of engineered nanoparticles in water: case studies from fullerene C_{60} nanoparticles and carbon nanotubes. *Environ. Chem.* **2010,** *7,* 10-27.
18. Chen, K. L.; Elimelech, M. Influence of humic acid on the aggregation kinetics of fullerene (C_{60}) nanoparticles in monovalent and divalent electrolyte solutions. *J. Colloid Interface Sci.* **2007,** *309,* 126-134.
19. Qu, X.; Hwang, Y. S.; Alvarez, P. J. J.; Bouchard, D.; Li, Q. UV irradiation and humic acid mediate aggregation of aqueous fullerene (nC_{60}) nanoparticles. *Environ. Sci. Technol.* **2010,** *44,* 7821-7826.

20. Xie, B.; Xu, Z.; Guo, W.; Li, Q. Impact of natural organic matter on the physicochemical properties of aqueous C_{60} nanoparticles. *Environ. Sci. Technol.* **2008,** *42,* 2853-2859.
21. Bouchard, D.; Ma, X.; Isaacson, C. Colloidal properties of aqueous fullerenes: Isoelectric points and aggregation kinetics of C_{60} and C_{60} derivatives. *Environ. Sci. Technol.* **2009,** *43,* 6597-6603.
22. Chen, K. L.; Elimelech, M. Interaction of fullerene (C_{60}) nanoparticles with humic acid and alginate coated silica surfaces: Measurements, mechanisms, and environmental implications. *Environ. Sci. Technol.* **2008,** *42,* 7607-7614.
23. Praetorius A, Arvidsson R, Molander S, Scheringer M. 2013. Facing complexity through informed simplifications: A research agenda for aquatic exposure assessment of nanoparticles. *Environ Sci Process Impacts* 15:161-168.
24. Chen, C. Y. and C. T. Jafvert Sorption of buckminsterfullerene (C60) to saturated soils. Environ. Sci. Technol. **2009,** *43(19)*: 7370-7375.
25. Wang, Y., Y. Li, et al. Transport and retention of fullerene nanoparticles in natural soils. J.Environ. Qual. **2010,** *39(6)*: 1925-1933.
26. Zhang, L., L. Hou, et al. Transport of fullerene nanoparticles (nC60) in saturated sand and sandy soil: Controlling factors and modeling. Environ. Sci. Technol. **2012,** *46(13)*: 7230-7238.
27. Kolkman A, Emke E, Bäuerlein PS, Carboni A, Tran DT, Ter Laak TL, van Wezel A, de Voogt P. 2013. Analysis of (functionalized) fullerenes in water samples by liquid chromatography coupled to high resolution mass spectrometry. *Anal Chem* DOI: 10.1021/ac400619g.
28. van Wezel, A. P.; Moriniere, V.; Emke, E.; ter Laak, T.; Hogenboom, A. C. Quantifying summed fullerene nC_{60} and related transformation products in water using LC LTQ Orbitrap MS and application to environmental samples. *Environ. Int.* **2011,** *37,* 1063-1067.
29. Huffman, D. R. Solid C_{60}. *Phys Today* **1991,** *44,* 22-29.
30. Chen, K. L.; Elimelech, M. Aggregation and deposition kinetics of fullerene (C_{60}) nanoparticles. *Langmuir* **2006,** *22,* 10994-11001.
31. Brant, J. A.; Labille, J.; Bottero, J. Y.; Wiesner, M. R. Characterizing the impact of preparation method on fullerene cluster structure and chemistry. *Langmuir* **2006,** *22,* 3878-3885.
32. Mashayekhi, H.; Ghosh, S.; Du, P.; Xing, B. Effect of natural organic matter on aggregation behavior of C_{60} fullerene in water. *J. Colloid Interface Sci.* **2012,** *374,* 111-117.
33. Isaacson, C. W.; Bouchard, D. C. Effects of humic acid and sunlight on the generation and aggregation state of *aqu*/C_{60} nanoparticles. *Environ. Sci. Technol.* **2010,** *44,* 8971-8976.
34. Dutch Government, http://live.waterbase.nl. *February, 2013.*
35. Klavins, M.; Ansone, L. Study of interaction between humic acids and fullerene C_{60} using fluorescence quenching approach. *Ecol. Chem. Eng. S.* **2010,** *17,* 351-362.
36. Pakarinen, K.; Petersen, E. J.; Alvila, L.; Waissi-Leinonen, G. C.; Akkanen, J.; Leppänen, M. T.; Kukkonen, J. V. K. A screening study on the fate of fullerenes (nC_{60}) and their toxic implications in natural freshwaters. *Environ. Toxicol. Chem.* **2013,** *32,* 10.1002/etc.2175.
37. Gallé T, Grégoire C, Wagner M, Bierl R. 2005. Bioavailability of HOC depending on the colloidal state of humic substances: A case study with PCB-77 and Daphnia magna. *Chemosphere* 61:282-292.
38. Gottschalk, F.; Nowack, B. The release of engineered nanomaterials to the environment. *J. Environ. Monitor.* **2011,** *13,* 1145-1155.
39. Jia M, Li H, Zhu H, Tian R, Gao X. 2013. An approach for the critical coagulation concentration estimation of polydisperse colloidal suspensions of soil and humus. *J Soil Sediment* 13:325-335.
40. Westerhoff P, Nowack B. 2013. Searching for global descriptors of engineered nanomaterial fate and transport in the environment. *Acc Chem Res* 46:844-853.
41. Quik JTK, Vonk JA, Hansen SF, Baun A, Van De Meent D. 2011. How to assess exposure of aquatic organisms to manufactured nanoparticles? *Environ Int* 37:1068-1077.

6 Appendices

6.1 Distribution of fullerenes between vials, filter, and suspension

The vials and membrane filters used in the preparation of the fullerene suspensions were extracted with toluene to calculate the losses of C_{60} and C_{60}BisPCBM to the glass wall and the filter material. A volume of about 3-4 mL of toluene was added to each vial (×16). The membrane filter was added to a clean vial and 10 mL of toluene was added. The vials were subsequently placed for 15 minutes on a Stuart Roller Mixer SRT9D (Staffordshire, United Kingdom). Organic solvent from all vial extractions was collected and each vial was rinsed with 2×0.5-1 mL of toluene. The vial and filter extracts were evaporated to about 1 mL with N_2 gas in a water bath held at 55 °C, and were added to volumetric flasks of 10 mL. Dilutions of 1:500 and 1:15 for the vial/filter extracts and the suspension, respectively, were measured with LC-Orbitrap MS to calculate the recovery. The amounts recovered from vials, filter, and suspension were 87% for C_{60} and 85% for C_{60}BisPCBM. The amounts sorbed to the glass wall of the vials, retained on the filter and suspended in solution were 32%/32%/23% for C_{60} and 40%/8%/37% for C_{60}BisPCBM.

6.2 Flow-field-flow fractionation

A volume of 100 μL of sample was injected into a thin channel of water flowing over a membrane (10 kDa regenerated cellulose, Postnova) with Milli-Q as eluent. At the moment of injection, the sample was focused into a small laminar band by opposing flows. After the focus flow of 1 mL/min. stopped after 5 min., the cross-flow (1 mL/min.) exponentially decreased to 0.1 mL/min. at 46 min. resulting in a higher retardation of large size components.

Separation in asymmetric flow-field-flow fractionation is achieved according to molar mass or particle size by interaction between a channel flow which carries the sample and a perpendicular cross-flow that creates a viscous force along the membrane and drags the sample to the membrane surface [1]. Individual species with specific diffusion or size properties equilibrate into zones that are created by the cross-flow field. Large components with low diffusivities therefore travel more slowly than small components with high diffusivities. The particle diameter is subsequently measured with a multi-angle light scattering (MALS) detector. The MALS detector measures light scattering from a multitude of 21 detectors surrounding a flow-through sample cell. The amount of light scattered from each angle is calculated and converted to an absolute molar mass or (exact) diameter of a particle. The refractive index increment (dn/dc in mL/g) is used as an input parameter in the calculation of particle radii. This parameter was approximated by taking the difference between the refractive index of solid fullerene (n = 2.20 measured at 630 nm and unknown temperature; [2]) and water (n = 1.333 at 589 nm and 20 °C;[3]) and subsequently dividing by the density of fullerene (1.65 g/cm^3). Thus, a refractive index increment of 0.525 mL/g was used for the determination of particle radii of nC_{60} and nC_{60}BisPCBM. However, small changes in the refractive index and density of C_{60}BisPCBM compared to that of C_{60} may affect the results.

6.3 Dynamic light scattering

In dynamic light scattering, fluctuations of photons that are scattered by particles due to constructive and destructive interference are measured in time. The frequency of these fluctuations is related to the temperature dependent Brownian motion of the particles in solution. The decay of the intensity of the scattered light is analyzed by fitting a second

order correlation function to the data (CONTIN algorithm). The decay rate corresponds to specific diffusivities of differently sized particles that are subsequently converted to a hydrodynamic size distribution through the Stokes-Einstein equation: $d = kT/3\pi\eta D$, where d is the particle diameter, k is the Boltzmann constant, T is the absolute temperature, η is the solvent viscosity, and D is the diffusion coefficient.

6.4 Electrophoretic mobility measurements

The electrophoretic mobility was determined with phase analysis light scattering which measured the phase shift of the scattered light depending on the velocity of the particles. With this technique, scattered light intensity at an angle of 17° is compared to a reference beam which produces light intensity fluctuations. The rate of these fluctuations is related to the velocity of the particles. The zeta potential is subsequently calculated by applying Henry equation ($U_E = 2\varepsilon z f(K_a)/3\eta$, where U_E is the electrophoretic mobility, ε is the dielectric constant, and z is the zeta potential) using Smoluchowski approximation, $f(K_a) = 1.5$, for water with moderate electrolyte concentrations.

6.5 Figures

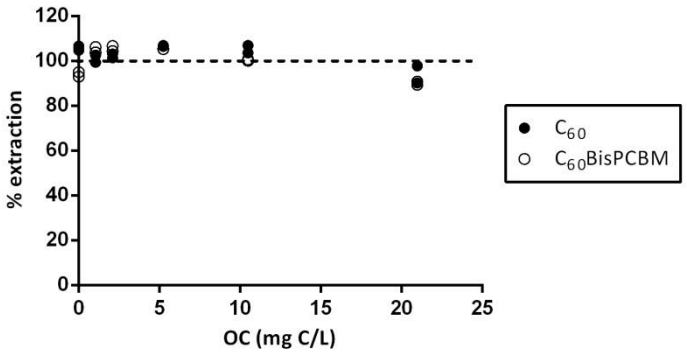

Figure S1. Extraction recovery of nC_{60} and nC_{60}BisPCBM from an aqueous solution in the presence of Leonardite humic acid.

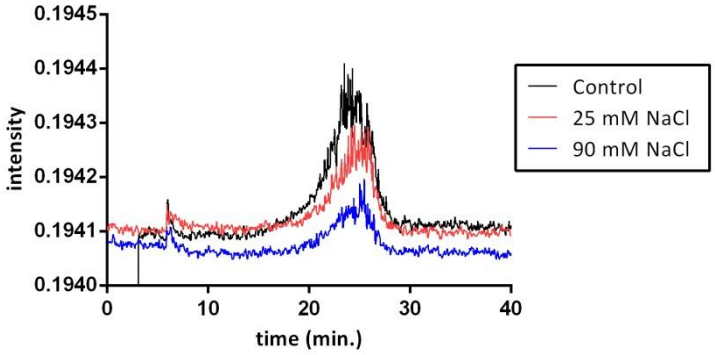

Figure S2. Effect of the presence of NaCl on the intensity of nC_{60} (~100 μg/L) measured with AF4-MALS (signal measured at an angle of 92°).

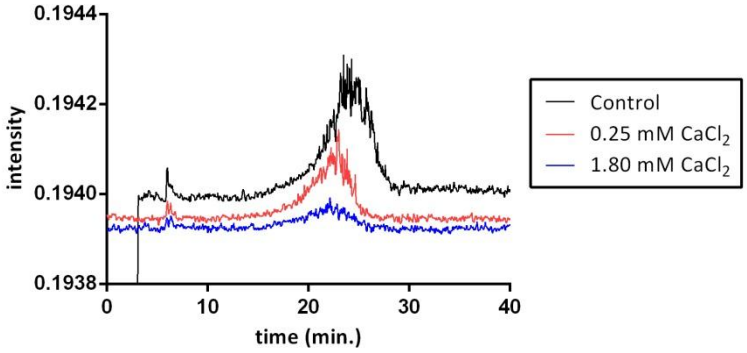

Figure S3. Effect of the presence of $CaCl_2$ on the intensity of nC_{60} (~100 μg/L) measured with AF4-MALS (signal measured at an angle of 92°).

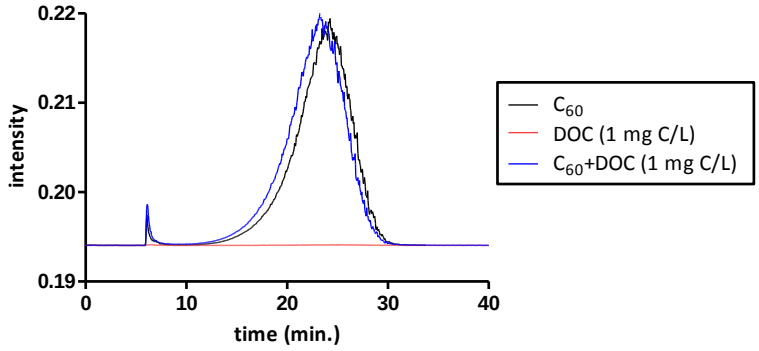

Figure S4. Effect of the presence of DOC on the intensity of C_{60} (concentration unknown) measured with AF4-MALS (signal measured at an angle of 92°).

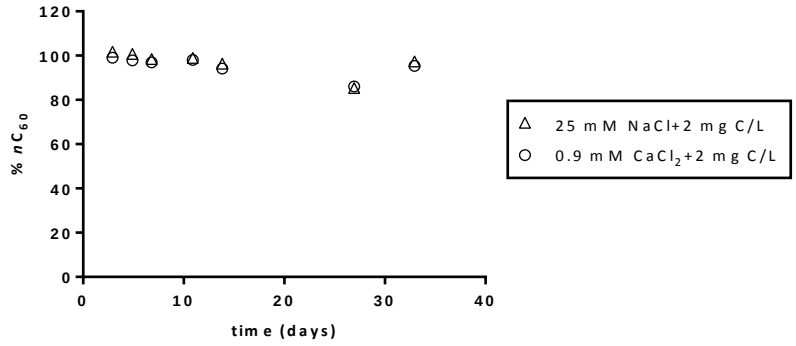

Figure S5. Effect of the presence of DOC and electrolytes on the colloidal stability of nC_{60} as a function of time.

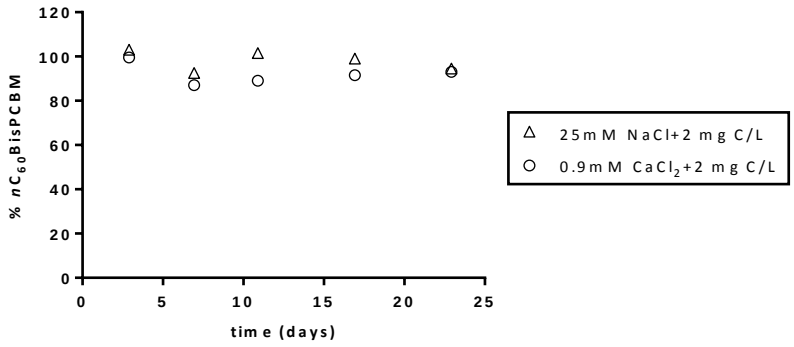

Figure S6. Effect of the presence of DOC and electrolytes on the colloidal stability of nC_{60}BisPCBM as a function of time.

6.6 Literatuur

1 Giddings JC. 1993. Field-flow fractionation: Analysis of macromolecular, colloidal, and particulate materials. *Science* 260: 1456-1465

2 Huffman DR. 1991. Solid C_{60}. *Phys Today* 44:22-29.

3 Hecht E. 2002. *Optics*. Pearson Higher Education, San Franciso, CA, USA.

6.7 Acknowledgements

Katarzyna Zielińska from the Laboratory of Physical Chemical and Colloid Science (Wageningen University) is acknowledged for the particle size and electrophoretic mobility measurements. This project was funded by the Dutch government via NanoNextNL and by the joint research program of the Dutch drinking water companies (BTO).